PHYSICAL REVIEW A VOLUME 15, NUMBER 4 APRIL 1977

Improved model for parallel-plate drift-tube experiments

J. H. Whealton,* D. S. Burch,† and A. V. Phelps‡
Joint Institute for Laboratory Astrophysics, University of Colorado and National Bureau of Standards, Boulder, Colorado 80309
(Received 15 November 1976)

The validity of analysis of parallel-plate drift-tube experiments by use of diffusion theory is examined. Monte Carlo simulations demonstrate the inadequacy of such analyses for electron motion near an absorbing cathode. However, diffusion theory results are verified for situations in which cathodic absorption is negligible, provided that a parameter β, the ratio of energy relaxation distance to drift-tube length, is much smaller than unity. For experimental circumstances in which cathode effects may be distinguished from those of anodic absorption, circuit time constant, and ionization, the Monte Carlo results can be used to augment diffusion theory for interpretation of the observed transients in terms of transport coefficients.

I. INTRODUCTION

In this paper we discuss the analysis of pulsed parallel-plate swarm experiments. There are two versions of the experiment that we have in mind: (i) electrons are ejected photoelectrically from a plane cathode,[1] or (ii) electrons are admitted to the drift space from a source region by means of a pulsed shutter which then acts as the equipotential cathode plane.[2] In either case the circuit current is observed by the potential difference generated across an external resistance, and the over-all circuit response time is usually made very large or very small compared to one drift-time interval. The purpose of the experiments is to provide data, the current transients, which may be interpreted in terms of transport parameters. In some cases the interpretation is hampered by such phenomena as secondary emission, attachment, lateral diffusion, and ionic motion,[3] none of which will be considered in this paper. On the other hand, effects due to longitudinal diffusion, absorption of electrons by the electrodes, and the circuit response time usually are ineluctable, as are also effects due to avalanche growth in many cases of interest. The roles played by these phenomena in the determination of the details of the transient waveform must be understood before a secure interpretation of the data is possible. One aim of this paper is to elucidate these roles.

In the limit $\beta \to 0$, where β is the ratio of the electron energy relaxation distance ($D_{\|}/v_d$) to the drift length h, and for circuit response time RC either much greater than a drift time (h/v_d) or much smaller, electron drift velocities may easily be extracted from the data.[4] Here, $D_{\|}$ is the longitudinal diffusion coefficient, v_d is the electron drift velocity, and R and C are the circuit resistance and capacitance, respectively. To determine the modifications to be expected from a finite value of β, numerous workers[5-7] have employed diffusion theory for cases with RC much smaller than the energy relaxation time. The starting point of these developments is a δ-function pulse of electrons at or near the cathode plane, with the electrons already possessed of the drift velocity and mean energy that will obtain in equilibrium with the electric field E and gas concentration N. If the cathode is treated as nonreflecting, it is also necessary to start the pulse at some distance from the cathode to avoid immediate reabsorption of the pulse. The criteria for choosing the initial conditions for the closest representation of the experimental circumstances are not precise, nor is it evident that such devices can give accurate results in the best use of them. On the other hand, a Monte Carlo simulation has been performed[8] in which cathode effects are neglected, and these calculations give results in agreement to order β with diffusion theory (neglecting cathode effects).

In this paper we will develop the diffusion theory of the transient waveform including anodic, circuit, and ionization effects, and then present a technique for the correction of the results to account for back diffusion to the cathode. The technique employs the result of Monte Carlo simulation for the early stages of the transient to estimate the concentration pulse distortion and displacement due to the presence of the absorbing cathode in cases where these effects can be separated from others. Finally, we will present some results for cases in which the various errors cannot be decoupled.

The basic experiment is illustrated in Fig. 1. Charged carriers are emitted from one of the electrodes and are accelerated by the electric field $E = V/h$ and hindered by collisions with the neutral gas molecules. A potential drop is generated across the resistance, and the time dependence of this signal is used to deduce the behavior of the charge carriers in the tube. This deduction

proceeds first from an elementary circuit analysis which considers the parallel current source shown by the dashes in Fig. 1. The current source shown $i(t)$ is due to the motion of the charged carriers,

$$i(t) = eA \int_0^h n(z,t)\langle v(E,z,t)\rangle\, dz, \tag{1.1}$$

where e, n, $\langle v_z\rangle$, and A are the carrier charge, concentration, average z component of carrier velocity, and effective cross-sectional area of the swarm, respectively. The integration is over the length of the discharge region.

Consideration of the voltages around the major loop in Fig. 1 yields

$$RC\frac{dI(t)}{dt} + I(t) = i(t), \tag{1.2}$$

which is not as trivial as it may appear; in general, $i(t)$ depends on $\langle v_z\rangle$, which depends on E, which depends in turn on I, making (1.2) nonlinear. Therefore, experimental conditions are usually chosen such that the voltage across the tube is negligibly changed during the transient,

$$i \ll V/R, \tag{1.3}$$

or the change of charge on a capacitor plate is negligible compared with the initial charge,

$$\Delta Q \ll Q_0. \tag{1.4}$$

The solution of Eq. (1.2), assuming the capacitor to be fully charged when the transient is initiated, $Q_0 = CV$, is[4]

$$I = \frac{1}{RC} e^{-t/RC} \int_0^t i(t') e^{t'/RC}\, dt'. \tag{1.5}$$

As mentioned above, the phenomena which must be incorporated in the evaluation of Eq. (1.5) will be considered in stages: in Sec. II we present the development of Eq. (1.5) by diffusion analysis, and then extend that development in Sec. III to account for anodic effects, ionization, and circuit time constant. In Sec. IV the consequences of cathodic phenomena are investigated by employing results from Monte Carlo calculations. In some cases the consequences of all these phenomena are simply cumulative and can be combined as is done in Sec. V to provide a basis for interpretation of experimental results (if the conditions of our model are otherwise met). However, there are circumstances in which the cathodic effects cannot be decoupled, and in Sec. VI we have used Monte Carlo calculations to provide examples which give insight into the behavior of the system in these cases.

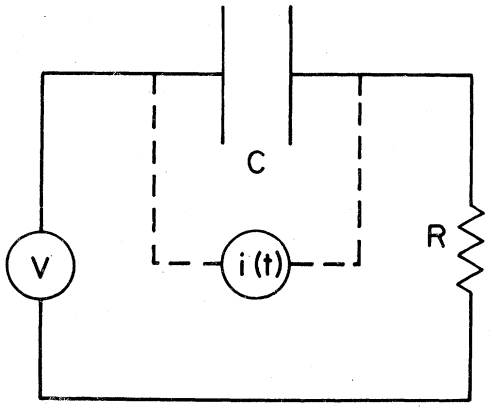

FIG. 1. Basic experiment and equivalent circuit.

II. DIFFUSION ANALYSIS

In this diffusion approximation,[9] Eq. (1.1) is evaluated by noting that

$$n\langle \vec{v}\rangle = n\vec{v}_d - \vec{D}\cdot\nabla n, \tag{2.1}$$

where the drift velocity and diffusion tensor are denoted by $\vec{v}_d$ and $\vec{D}$, respectively. The electron density n is evaluated by considering Eq. (2.1) along with the equation of continuity

$$\frac{\partial n}{\partial t} + \nabla\cdot n\langle \vec{v}\rangle = \nu n,$$

where ν is the ionization frequency, which yields

$$\frac{\partial n}{\partial t} + \vec{v}_d\cdot\nabla n - \vec{D}:\nabla\nabla n = \nu n. \tag{2.2}$$

We will consider only net motion in the direction of the electric field, which implies that radial diffusion of ions or electrons out of the drift space is ignorable, thus restricting applications of the model to experiments performed with drift tubes which are wide relative to the drift length on a scale determined by the ratio of the transverse diffusion coefficient to the mobility of electrons in the gas being studied.

It is convenient to form dimensionless quantities in this analysis; therefore all times are scaled by the time it takes for the ions to drift across the tube and all distances by the length of the drift tube:

$$\tau \equiv tv_d/h, \quad \xi \equiv z/h, \quad rc \equiv RCv_d/h, \quad \beta \equiv D_{\|}/v_d h,$$
$$\gamma \equiv \nu h/v_d, \quad \eta = nhA, \quad j = I/ev_d. \tag{2.3}$$

Physically, rc is the ratio of the circuit time constant to the drift time, γ is the number of ionization events per electron in a drift time, β is the ratio of an energy relaxation distance to the drift-tube length.

Now the system of equations we wish to consider is the first-order circuit equation (1.2)

$$rc\frac{\partial j}{\partial \tau}+j(\tau)=i(\tau), \tag{2.4}$$

where from Eq. (1.1)

$$i(\tau)=\int_0^1 d\xi\left(\eta-\beta\frac{\partial\eta}{\partial\xi}\right)$$

$$=\int_0^1 \eta\,d\xi-\beta\eta(1)+\beta\eta(0), \tag{2.5}$$

and, from Eqs. (2.2),

$$\frac{\partial\eta}{\partial\tau}+\frac{\partial\eta}{\partial\xi}-\beta\frac{\partial^2\eta}{\partial\xi^2}=\gamma n. \tag{2.6}$$

The solution to Eqs. (2.4)–(2.6) is found in Appendix A to be

$$j(\tau)=\int_{-\infty}^{+\infty} d\xi\,\eta(\xi,0)G(\xi,\tau),$$

where the Green's function is

$$G(\xi,\tau)=\frac{e^{-\tau/rc}}{1+\gamma rc}\left[\frac{(1+\sigma)^2}{8\sigma}\exp\left(\frac{1-\sigma}{2\beta}(1-\xi)\right)\operatorname{erfc}\left(\frac{1-\xi-\sigma\tau}{\sqrt{4\beta\tau}}\right)\right.$$

$$\left.-\frac{(1-\sigma)^2}{8\sigma}\exp\left(\frac{1+\sigma}{2\beta}(1+\xi)\right)\operatorname{erfc}\left(\frac{1-\xi+\sigma\tau}{\sqrt{4\beta\tau}}\right)-1\right]+\frac{e^{\gamma\tau}}{2(1+\gamma rc)}\operatorname{erfc}\left(\frac{\tau+\xi-1}{\sqrt{4\beta\tau}}\right). \tag{2.7}$$

Here

$$\sigma\equiv(1-4\beta\gamma-4\beta/rc)^{1/2}$$

and

$$\mathrm{Re}(\sigma)\leq 1, \tag{2.8}$$

or equivalently $\gamma\geq -1/rc$. Equation (2.8) poses no restriction on ionization processes ($\gamma>0$), only on depletion processes, which we will not discuss. The restriction arises from consideration of a particular configuration of poles in the evaluation of Eq. (2.7). The initial conditions to be inserted into Eq. (2.7) are not yet specified and are a complication outside the scope of diffusion theory and so require a different type of analysis as discussed in Sec. III.

III. EFFECTS OF ANODE, IONIZATION, AND TIME CONSTANT

To take account of an absorbing anode boundary at $\xi=1$, we may add an image to the initial conditions[5,10,11]

$$\eta_{ABC}(\xi,0)=\eta_{OBC}(\xi,0)-e^{1/\beta}\eta_{OBC}(2-\xi,0), \tag{3.1}$$

which suffices to make the density zero at $\xi=1$ for all time and enables us to use the Green's function (2.7). The current in the external circuit for a $\delta(\xi)$ initial carrier density distribution is

$$j(\tau)=\frac{e^{-\tau/rc}}{1+\gamma rc}\left[\frac{(1+\sigma)^2}{8\sigma}\exp\left(\frac{1-\sigma}{2\beta}\right)\operatorname{erfc}\left(\frac{1-\sigma\tau}{\sqrt{4\beta\tau}}\right)-\frac{(1-\sigma)^2}{8\sigma}\exp\left(\frac{1+\sigma}{2\beta}\right)\operatorname{erfc}\left(\frac{1+\sigma\tau}{\sqrt{4\beta\tau}}\right)-1\right]+\frac{e^{\gamma\tau}}{2(1+\gamma rc)}\operatorname{erfc}\left(\frac{\tau-1}{\sqrt{4\beta\tau}}\right) \tag{3.2}$$

for no anode boundary condition, and

$$j(\tau)=\frac{e^{-\tau/rc}}{1+\gamma rc}\left[\tfrac{1}{2}\exp\left(\frac{1-\sigma}{2\beta}\right)\operatorname{erfc}\left(\frac{1-\sigma\tau}{\sqrt{4\beta\tau}}\right)+\tfrac{1}{2}\exp\left(\frac{1+\sigma}{2\beta}\right)\operatorname{erfc}\left(\frac{1+\sigma\tau}{\sqrt{4\beta\tau}}\right)-1\right]$$

$$+\frac{e^{\gamma\tau}}{2(1+\gamma rc)}\operatorname{erfc}\left(\frac{\tau-1}{\sqrt{4\beta\tau}}\right)-\frac{e^{\gamma\tau+1/\beta}}{2(1+\gamma rc)}\operatorname{erfc}\left(\frac{\tau+1}{\sqrt{4\beta\tau}}\right) \tag{3.3}$$

for an absorbing anode. Equations (3.2) and (3.3) are subject to $\gamma\geq -1/rc$ as is (2.7), from mathematical considerations, as well as $\beta\ll 1$ and $4\gamma\beta\leq 1$ from physical considerations.[12]

Solutions to Eqs. (3.2) and (3.3) are shown in Fig. 2 illustrating the effect of the external circuit time constant rc in a case where ionization is absent, $\lambda=0$, and diffusion is small, $\beta=10^{-2}$. Either Eq. (3.2) or (3.3) gives the same result to order β^2.

In the limit of small time constant, i.e., $rc\ll(\beta,\gamma,\tau,1)$, Eqs. (3.2) and (3.3) become, respectively,[6,13]

$$j(\tau)=\tfrac{1}{2}e^{\gamma\tau}\left[\operatorname{erfc}\left(\frac{\tau-1}{\sqrt{4\beta\tau}}\right)-\left(\frac{\beta}{\pi\tau}\right)^{1/2}\exp\left(-\frac{(1-\tau)^2}{4\beta\tau}\right)\right] \tag{3.4}$$

and[5,14,15]

$$j(\tau)=\tfrac{1}{2}e^{\gamma\tau}\left[\operatorname{erfc}\left(\frac{\tau-1}{\sqrt{4\beta\tau}}\right)-e^{1/\beta}\operatorname{erfc}\left(\frac{1+\tau}{\sqrt{4\beta\tau}}\right)\right] \tag{3.5}$$

Lowke[5] also considers no absorbing anode as in the case of Eq. (3.4) but neglects a boundary term [Eq. (19) of Ref. 5] which gives rise to the last

term in Eq. (3.4). Therefore his result [Eq. (21) of Ref. 5] excludes this term and gives rise to a larger difference between an absorbing and nonabsorbing anode than we obtain. His results are shown in Fig. 4 of Ref. 5 which are quite different from Fig. 3, herein, showing the importance of keeping the boundary terms and showing the very minor influence of the anode in the pulsed parallel plate experiment. Figure 4 of Ref. 5 can be seen to contain an error without the help of the above arguments by simply noting that the area under the transient curves is different for the absorbing and nonabsorbing anode. The total charge collected and thus the total area under the current curve for any given electron pulse should be the same for both cases.

When small ionization and diffusion,[5-7,13-15] i.e., $rc \ll (\beta,\gamma) \ll (1,\tau)$, are also considered, Eqs. (3.4) and (3.5) become, respectively,

$$j(\tau)=\tfrac{1}{2}\operatorname{erfc}\left(\frac{\tau-1}{\sqrt{4\beta\tau}}\right)-\left(\frac{\beta}{4\pi\tau}\right)^{1/2}\exp\left(-\frac{(1-\tau)^2}{4\beta\tau}\right) \tag{3.6}$$

and

$$j(\tau)=\tfrac{1}{2}\operatorname{erfc}\left(\frac{\tau-1}{\sqrt{4\beta\tau}}\right)-\frac{1}{1+\tau}\left(\frac{\beta\tau}{\pi}\right)^{1/2}\exp\left(-\frac{(1-\tau)^2}{4\beta\tau}\right). \tag{3.7}$$

Solution to Eqs. (3.4)–(3.7) are shown in Fig. 3 for the case of no ionization, $\gamma=0$. Within plotting accuracy, all four equations give the same result for $\beta \leq 0.03$. For $\beta \geq 0.1$ Eqs. (3.4) and (3.5) yield a difference, as shown in Fig. 3, and Eqs. (3.6) and (3.7) are inaccurate; however, in this case the diffusion analysis is suspect.[8] For $\beta \leq 0.003$ Eq. (3.7) is far easier to use than Eq. (3.5) because the latter involves products of very large and very small numbers.

In the limit of long rise time, as well as small ionization and diffusion, i.e., $(\beta,\gamma) \ll (1,\tau) \ll rc$,

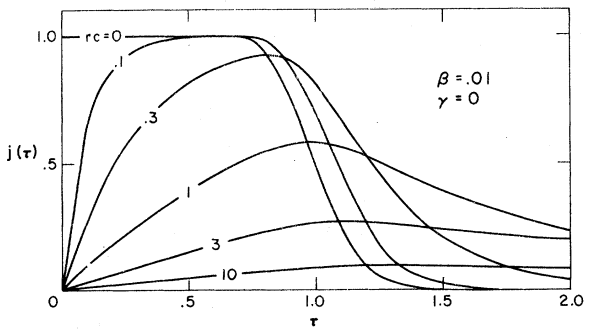

FIG. 2. Transient current illustrating effect of rise time with small diffusion and zero ionization from Eqs. (3.2)–(3.5).

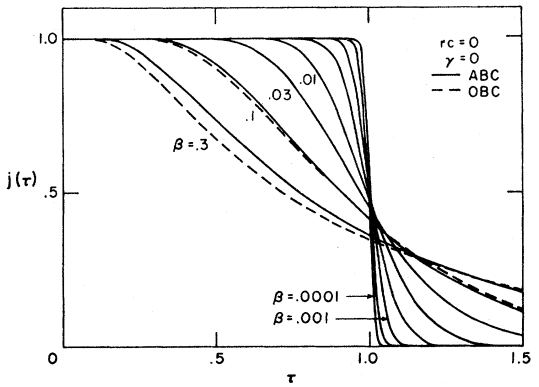

FIG. 3. Transient current illustrating effect of diffusion and absorbing anode for zero rise time and ionization. The solid lines refer to solution of Eq. (3.5) or (3.7) with an absorbing anode boundary condition, denoted as ABC. The dashed line refers to solution of Eq. (3.4) or (3.6) with no anode boundary condition, denoted as OBC.

Eqs. (3.2) and (3.3) both reduce to

$$j(\tau)=\frac{1}{rc}\left[\tau+\left(\frac{1-\tau}{2}\right)\operatorname{erfc}\left(\frac{1-\tau}{\sqrt{4\beta\tau}}\right)-\left(\frac{\beta\tau}{\pi}\right)^{1/2}\exp\left(-\frac{(1-\tau)^2}{4\beta\tau}\right)\right]. \tag{3.8}$$

Solution to Eq. (3.8), as well as Eqs. (3.2) and (3.3) for $rc=10^4$, is shown in Fig. 4 for the case of no ionization, $\gamma=0$. For $\beta \leq 0.1$, no significant difference is obtained from Eqs. (3.2) and (3.3) due to an absorbing anode. Equation (3.8) can be used in place of Eq. (3.2) or (3.3) in this case, to plotting accuracy of this figure, for $\beta \leq 0.03$ and is recommended for computational convenience for $\beta \leq 0.003$.

The effect of ionization ($\gamma > 0$) is shown in Fig. 5 for the short [Eq. (3.4) or (3.5)] or long [Eq.

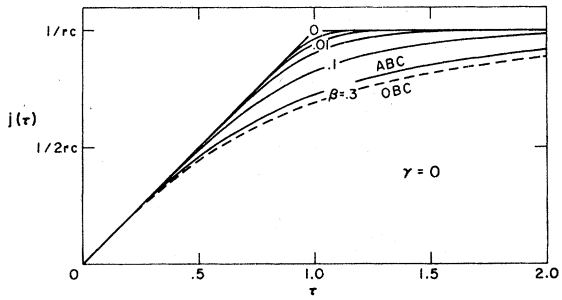

FIG. 4. Transient current illustrating effect of diffusion and absorbing anode for very large rise time and zero ionization. The solid lines refer to solution to Eq. (3.3) or (3.8) with an absorbing anode boundary condition, denoted as ABC. The dashed line refers to solution of Eq. (3.2) or (3.8) with no anode boundary condition, denoted as OBC.

(3.2) or (3.3), with $rc = 10^4$] rise time case with small diffusion ($\beta = 10^{-2}$) for ionization significantly less than the back diffusion breakdown criterion[12] ($\gamma = 25$).

Finally, in the absence of diffusion, i.e., $0 = \beta \ll (rc, \gamma, \tau, 1)$, Eqs. (3.2) and (3.3) both reduce to[16]

$$j(\tau) = \frac{1}{1+\gamma rc} \times \begin{cases} (e^{\gamma\tau} - e^{-\tau/rc}), & \tau < 1, \\ e^{-\tau/rc}(e^{\gamma+1/rc} - 1), & \tau > 1. \end{cases} \quad (3.9)$$

Most of the analyses of the pulsed parallel-plate experiment do not consider diffusion, but those that do, consider only the limit of fast response time, i.e., $rc \ll \beta, \gamma, \tau, 1$. In addition, usually at most one absorbing boundary is considered,[5,11,13-15] with the exception of one recent attack by the image method that considers both boundaries absorbing and has the initial ions infinitesimally close to the cathode.[7] Some unpublished work[6] considers absorbing boundaries by solving the relevant eigenvalue problem. There also exists some work[17] considering two absorbing boundaries, which we believe to be faulty. These points are discussed further in Appendices B–D.

In this section we have assumed that cathode and other effects are decoupled and that the initial density distribution is a $\delta(\xi)$ function. The latter condition is simply illustrative and can be bypassed with appropriate convolution over the results of Sec. IV, while the former restriction is the subject of Sec. VI. It is useful to separate cathode effects from the other considered effects of absorbing anode, diffusion, ionization, and circuit time constants since the methods used to deal with the latter effects are so different. In Sec. VI examples will be shown to illustrate when the cathode and other effects can not be decoupled. An alternate but inferior way of dealing with a cathode boundary condition is considered in Appendix B with connection to existing theories.

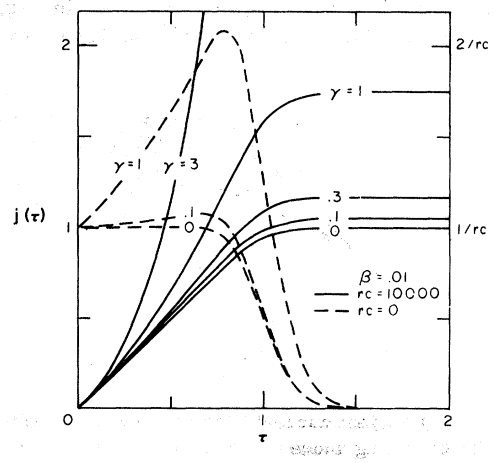

FIG. 5. Transient current illustrating effect of ionization for small diffusion, very short rise time (dotted line, vertical scale at the left-hand side) and very large rise time (solid line, vertical scale at the right-hand side) from Eqs. (3.2)–(3.3).

IV. CATHODE EFFECTS

A Monte Carlo calculation, described elsewhere,[8] is used to simulate cathode effects. Principal assumptions are constant mean free time, isotropic scattering, $m \ll M$, and neglect of neutral motion. Electrons are ejected perpendicularly from the cathode with a velocity v_0 (in units of the drift velocity v_d). The effect of inelastic collisions is approximated by adjusting the mass ratio m/M appropriately.

Examples of the early time density distributions of electrons ejected from an absorbing cathode are shown in Fig. 6. The normalized densities are plotted against distance normalized by the drift distance. For a few collision times τ_c a free fall wave is visible governed by the applied electric field. The shaded bar in the wave front depicts the fraction of electrons in this wave or alternatively the number of electrons not yet having a collision. After ten or more collision times the front is far away and its population minute. The density distributions tend toward a Gaussian but

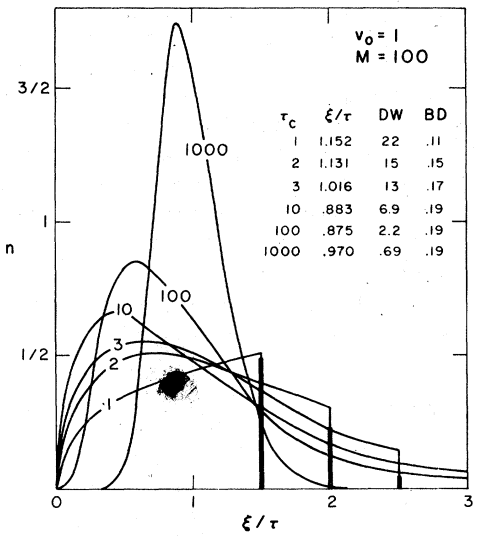

τ_c	ξ/τ	DW	BD
1	1.152	22	.11
2	1.131	15	.15
3	1.016	13	.17
10	.883	6.9	.19
100	.875	2.2	.19
1000	.970	.69	.19

FIG. 6. Monte Carlo renormalized electron density distribution ejected from an absorbing cathode for various times from 1 to 1000 collision times showing fraction back diffused and fraction of electrons in free fall wave (not yet having a collision). The electrons are all ejected perpendicularly from the cathode with a speed equal to the drift velocity and then have inelastic collisions with the neutrals equivalent to a mass ratio of 100. For $\tau_c < 3$, 10^5 electrons were considered and for $\tau_c \geq 3$, 10^4 electrons were considered.

are slightly skewed about the drift position, $\xi=\tau$, even after 1000 collision times or 30 energy relaxation times. The mean position, for this case, denoted by $\bar{\xi}/\tau$, is faster than the peak position but slower than the drift position, $\xi=\tau$, and approaches the drift position at long times. The diffusion equation solution for an initial δ-function density distribution in unbounded space would be a Gaussian whose mean is at $\xi=\tau$ and whose half-height width at the times and in the units indicated are shown in the column denoted by DW. The case considered in Fig. 6 is for electrons ejected perpendicularly from the cathode at a velocity equal to the drift velocity. The neutrals are taken to be 100 times heavier than the electrons. The fraction back diffusing (BD) is shown. In this case all that are going to back diffuse do so after a few collision times. The densities in Fig. 6 are renormalized at each time according to the number which have not yet back diffused.

In Fig. 7 is shown a more comprehensive set of density distributions after three energy relaxation distances for various initial speeds in units of the drift velocity v_0 and various mass ratios M/m. It is these distributions that may be taken as initial distributions to the diffusion analysis in Secs. II and III. Notice that the peak position and, to a smaller extent, the centroid may be either ahead or behind the drift position $\xi=\tau$ at this time, depending on the initial speed and mass ratio.

V. INTERPRETATION OF DECOUPLED EXPERIMENTS

The interpretation proceeds in two parts: errors due to cathode effects and errors due to other effects. The former, which are phrased in terms of aberrations in the density distribution, are additive to the latter, which are phrased in terms of aberrations in the external circuit current.

A. Incorporation of the effects of the cathode

Analytic asymptotic error formulas for cathode effects are not obtained since a suitable theory has not been developed (see Appendix B). Therefore recourse is made to the information available from Fig. 7. Figure 8 considers the position of the density centroid relative to the centroid due only to drift $3\beta(\delta-1)$ from the six cases considered in Fig. 7, interpolated to intermediate initial velocities and mass ratios. This procedure provides a basis for estimating errors in the drift velocity due to cathode effects. That is, owing only to cathode effects, the true drift velocity v_d is related to the apparent drift velocity v_d' by

$$v_d=v_d'(1-3\beta\delta), \tag{5.1}$$

where the factor 3β occurs because the data in Fig. 7 were taken at three energy relaxation times. Lowke[5] concludes, via diffusion analysis (see Appendix B), that $\delta=\frac{2}{3}$ as shown by the dashed line in Fig. 8, no matter what the initial velocity or mass ratio. Because only considerations of the density distribution are made in this section, the results are independent of rc time constants. Ionization is assumed to be negligible.

B. Other corrections

In this section we will not consider ionization and will separate the interpretation into cases

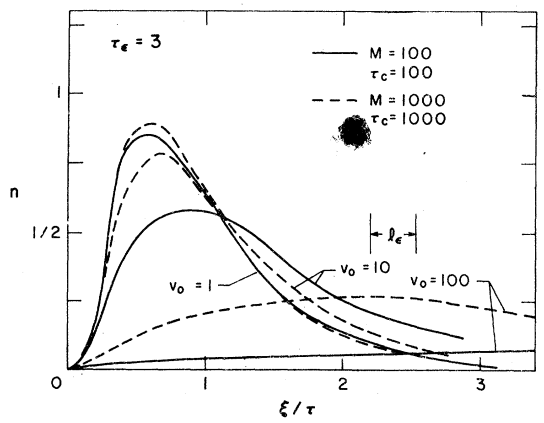

FIG. 7. Monte Carlo renormalized density distributions from an absorbing cathode at $3\tau_\epsilon$ for three initial speeds and two degrees of inelastic collisions with the neutrals. 10^4 electrons were considered. The drift distance at this time is at $\xi=\tau$.

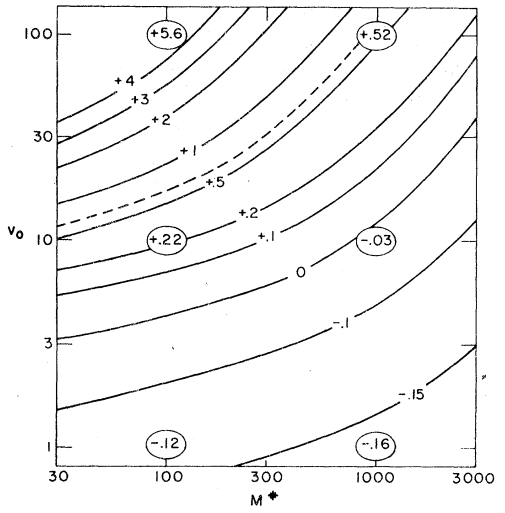

FIG. 8. Contours of δ, the cathode correction factor, used in Eq. (5.1) for consideration of cathode errors. These contours were obtained from the data shown in Fig. 7 by interpolation and extrapolation around the six points circled.

characterized by the time constant of the external circuit. For both extremely small time constants [for which Eqs. (3.4)–(3.7) are valid] or extremely large time constant [for which Eq. (3.8) is valid] a simple geometric interpretation of the arrival time spectra for obtaining the drift velocities is possible.

For the case of short rise times and small diffusion, i.e., $rc,\beta \ll 1$, from Eq. (3.9) and any of Eqs. (3.4)–(3.7) considering the apparent drift time to be the time at which the current is half the plateau value (see Fig. 3), the true drift velocity is derivable from the apparent drift velocity by the correction

$$v_d = v_d'[1 - \beta + rc \ln 2 + O(\beta^2, (rc)^2)], \qquad (5.2)$$

which should be combined with Eq. (5.1) to include cathode corrections. Equation (5.2) follows whether or not an absorbing anode boundary is imposed because the anode boundary effect is of $O(\beta^2)$ in this experiment.

For the case of large circuit rise times, i.e., $rc \gg 1$ as for Fig. 4, the intersection of the tangent of the current at $\tau \approx \frac{1}{2}$ and $\tau \approx \frac{3}{2}$ gives the drift time correction, which, from Eqs. (3.8) and (3.9), is

$$v_d = v_d'[1 - 1/8rc + O(1/(rc)^2, e^{-1/8})]. \qquad (5.3)$$

which should be combined with Eq. (5.1) to include cathode corrections.

For the case of intermediate rise times and $\beta \ll 1$, the current transient form should be fitted to Eq. (3.3) which, along with Eq. (5.1), will yield the drift velocity.

Diffusion coefficients are best obtained by fitting the data to Eqs. (3.3). For very short circuit response times, i.e., $rc \ll \beta \ll 1$, the data may be fitted to Eq. (3.7) (see Fig. 3) or one could use the fact that the slope of the current waveform at the apparent drift time is $-(4\pi\beta)^{-1/2}$. For very large circuit response time, i.e., $\beta \ll 1 \ll rc$, the data may be fitted to Eq. (3.8) (see Fig. 4) or one could use the fact that the slope of the current waveform at the apparent drift time is $[1 - (\beta/\pi)^{1/2}]/2rc$.

VI. COUPLING BETWEEN CATHODE AND OTHER EFFECTS

As in Sec. IV on cathode effects, the material in this section is not amenable to rigorous theoretical treatment (see Appendices C and D). Therefore, the Monte Carlo calculations are used, and for economic reasons we have restricted attention to an illustrative situation considered in Sec. III, i.e., $rc = \gamma = 0$.

The first example, illustrating a case where the absorbing cathode and other effects can marginally be separated, is shown in Fig. 9 in which $\beta = \frac{1}{30}$, $v_0 = 10$, $M/m = 100$. For this case there are about

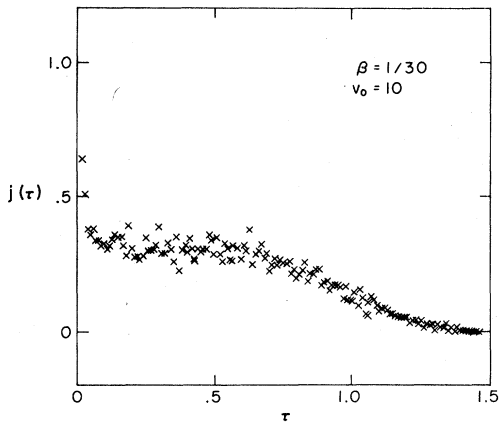

FIG. 9. Monte Carlo electron transient current illustrating marginally uncoupled cathode and anode absorption with large diffusion ($\beta = \frac{1}{30}$) for an initial speed ($\perp$ cathode) v_0 which is 10 times the drift velocity, for zero rise time, considering 10^4 electrons. The drift time is about 10^3 collision times and the degree of inelastic electron-neutral collisions is represented by a mass ratio of 100. These data are not renormalized to account for back diffusion.

1000 collision times in a transit time. At time $\tau = 0^+$, $j(0^+) = 10$. It rapidly $[\tau \sim O(\beta)]$ diminishes, due to back diffusion, to about $j \sim 0.3$ where a plateau region is formed lasting until $\tau \sim 0.6$. At later times most of the remaining carriers are absorbed by the anode. The crucial feature that enables us to separate cathode and other effects is the existence of the plateau region from $\tau = 0.3$ to 0.6. In this region carriers are not being significantly absorbed by either the cathode or the anode. For long rise time, as in Fig. 4, the analogous situation is that there exists a region (near $\tau \sim 0.2$) with constant slope. It is for experiments where there is a decoupling between cathode and other effects that we have, in Secs. I–V, presented results of sufficient generality to allow a meaningful interpretation.

The second example, illustrating a case where the absorbing cathode and other effects can not be separated, is shown in Fig. 10 in which $\beta = \frac{1}{3}$. Three different widely spaced initial velocities of ejection are considered, all of which greatly affect the fraction back diffused into the absorbing cathode but none of which allow a significant length of time in which carriers are not being simultaneously absorbed by both the cathode and anode.

ACKNOWLEDGMENTS

We wish to thank H.-C. Chen, C. Kunasz, and E. F. Jaeger for help in the numerical calculations and to S. B. Woo, H. R. Skullerud, I. R. Gatland, and E. A. Mason for their interest and helpful

discussions. This work was supported in part by the Advanced Research Projects Agency of the Department of Defense and was monitored by the U. S. Army Research Office under contract No. DAHC04-73-C-0029 and by the Office of Naval Research under contract No. N00014-67-A-0405-0008.

APPENDIX A: GREEN'S FUNCTION FOR THE CURRENT

We wish to solve Eqs. (2.4)–(2.6) in unbounded space for arbitrary initial conditions. To do this we consider the current induced in the external circuit j due just to carriers in the drift tube between ξ and $\xi+d\xi$. Then, the induced current due to all the carriers is

$$j(\tau)=\int_0^1 d\xi\, j(\xi,\tau)-\beta j(1,\tau)+\beta j(0,\tau), \tag{A1}$$

and the system of equations considered is

$$\frac{\partial j}{\partial \tau}+\frac{j}{rc}=\frac{\eta}{rc} \tag{A2}$$

and Eq. (2.6). In addition we assume that initially (before carriers enter the drift region) the circuit is in steady state so that before the carrier pulse is formed, $j(0^-)=j(\xi,0^-)=0$.

A Laplace-Fourier transform of Eqs. (A2) and (2.6) yields

$$\tilde{\bar{j}}=\frac{\tilde{\eta}(0)}{rc(s+1/rc)(s+ik+\beta k^2-\gamma)}, \tag{A3}$$

where s and k are the Laplace and Fourier transform parameters and $i=(-1)^{1/2}$. An inverse Laplace transform yields

$$\tilde{j}=\frac{\tilde{\eta}(0)}{rc}\left(\frac{\exp(-\tau/rc)-\exp[-\tau(\beta k^2+ik-\gamma)]}{\beta k^2+ik-1/rc-\gamma}\right). \tag{A4}$$

The inverse Fourier transform of Eq. (A4) is obtained by use of a double convolution theorem which reads

$$F^{-1}[\tilde{f}_1(k)\tilde{f}_2(k)\tilde{f}_3(k)]$$

$$=\frac{1}{(2\pi)^2}\int\int_{-\infty}^{+\infty} d\xi'\, d\xi''\, f_1(\xi-\xi'-\xi'')f_2(\xi')f_3(\xi''), \tag{A5}$$

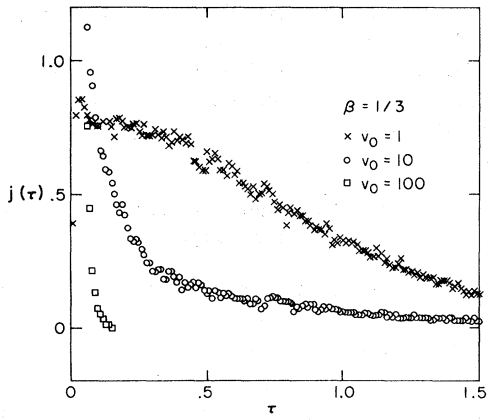

FIG. 10. Monte Carlo electron current illustrating coupled cathode and anode absorption with very large diffusion ($\beta=\frac{1}{3}$) for various initial speeds ($\perp$ cathode), for zero rise time, considering 2×10^4 electrons. The drift time is about 10^2 collision times and the degree of inelastic electron neutral collisions is represented by a mass ratio of 100. These data are not renormalized to account for back diffusion.

where

$$\tilde{f}_1=e^{-\tau/rc}-e^{-\tau(\beta k^2+ik-\gamma)}, \tag{A6}$$

$$\tilde{f}_2=\tilde{\eta}(0), \tag{A7}$$

$$\tilde{f}_3=(\beta k^2+ik-1/rc-\gamma)^{-1}. \tag{A8}$$

Therefore, inverse Fourier transformation yields

$$f_1=2\pi\delta(\xi)e^{-\tau/rc}-(\pi/\beta\tau)^{1/2}\exp[-(\xi-\tau)^2/\beta\tau+\gamma\tau], \tag{A9}$$

$$f_3=(4\pi/\sigma)e^{\xi/2\beta}\sinh(\sigma\xi/2\beta),\quad \xi<0$$
$$=0,\quad \xi\geq 0, \tag{A10}$$

where

$$\sigma\equiv(1-4\beta\gamma-4\beta/rc)^{1/2}. \tag{A11}$$

For the contour considered in the evaluation of Eq. (A8), $\mathrm{Re}\,\sigma\leq 1$. The result is

$$j(\xi,\tau)=\frac{e^{-\tau/rc}}{2rc\sigma}\int_{-\infty}^{+\infty} d\xi'\eta(\xi',0)\exp\left(\frac{(\xi-\xi')}{2\beta}\right)$$
$$\times\left[\exp\left(\frac{-\sigma|\xi-\xi'|}{2\beta}\right)\mathrm{erfc}\left(\frac{|\xi-\xi'|-\sigma\tau}{\sqrt{4\beta\tau}}\right)-\exp\left(\frac{\sigma|\xi-\xi'|}{2\beta}\right)\mathrm{erfc}\left(\frac{|\xi-\xi'|+\sigma\tau}{\sqrt{4\beta\tau}}\right)\right]. \tag{A12}$$

Substituting into Eq. (A1) taking the lower limit to be $-\infty$ instead of zero, Eq. (2.7) is obtained. A lower limit of $-\infty$ instead of zero takes care of meaningless artifacts introduced by the mathematics by not considering a cathode boundary explicitly.[5]

APPENDIX B: IMAGE DIFFUSION ANALYSIS WITH ABSORBING CATHODE

If an absorbing cathode boundary is considered in the diffusion approximation the initial condition inserted into Eq. (2.7), in analogy with Eq. (3.1), is[5,10,11]

$$\eta_{CBC}(\xi,0)=\eta_{OBC}(\xi-\epsilon,0)-e^{-\epsilon/\beta}\eta_{OBC}(\epsilon-\xi,0). \quad \text{(B1)}$$

The location ϵ of the initial density is not internally specified in the theory and it is natural to match the back diffusion predicted by diffusion theory with Eq. (B1), i.e., $e^{-\epsilon/\beta}$ for $\beta \ll 1$, to a suitable independent back diffusion theory. We shall use the Thompson-Leob theory[18] according to which the fraction back diffused is $(1+4/v_0)^{-1}$ and which implies $\epsilon=\beta \ln(1+4v_0)$. Thus the cathode correction factor predicted by use of the diffusion and Thompson-Leob theories is

$$\delta=-\ln[1+4v_0]/6v_0, \quad \text{(B2)}$$

which agrees with Lowke's[5] result, $\delta=\frac{2}{3}$, for $\epsilon, v_0 \ll \beta^2$. This result is not self-consistent. The Monte Carlo calculation, as is seen from Fig. 8, shows that the v_0 corresponding to $\delta=\frac{2}{3}$ does not generally result in $\epsilon \ll \beta$. Also from Eq. (B2) $\delta \to 0$ as $v_0 \to \infty$ which is obviously entirely wrong. Although the parameter ϵ can be adjusted to account for back diffusion, it must be recognized as an *ad hoc* parameter with no physical significance.

In order to connect with previous work on analyzing drift-tube experiments,[5-7,11,13-15,17] we shall indicate the results for three cases.

For very short rise times and small diffusion, i.e., $rc \ll \gamma, \epsilon, \beta \ll 1, \tau$, the current transient is

$$j(\tau)=\tfrac{1}{2}(1-e^{-\epsilon/\beta})\operatorname{erfc}\left(\frac{\tau-1}{\sqrt{4\beta\tau}}\right)-\left(\frac{\epsilon}{\sqrt{4\pi\beta\tau}}\right)\exp\left(-\frac{(1-\tau)^2}{4\beta\tau}\right). \quad \text{(B3)}$$

For intermediate rise time, i.e., $\gamma, \epsilon, \beta \ll 1, \tau, rc$, the current is

$$j(\tau)=(1-e^{-\epsilon/\beta})\left\{1-e^{-\tau/rc}+\tfrac{1}{2}\left[\exp\left(\frac{1-\tau}{rc}\right)-1\right]\operatorname{erfc}\left(\frac{1-\tau}{\sqrt{4\beta\tau}}\right)\right\}$$

$$-\frac{1}{rc}\left(\frac{\beta\tau}{\pi}\right)^{1/2}\left[\exp\left(\frac{1-\tau}{rc}-\frac{(1-\tau)^2}{4\beta\tau}\right)\right]\left\{(1+e^{-\epsilon/\beta})-(1+e^{-\epsilon/\beta})\frac{\epsilon rc}{2\beta\tau}\left[1+\exp\left(\frac{\tau-1}{rc}\right)\right]\right\}, \quad \text{(B4)}$$

and, for long rise times, i.e., $\gamma, \epsilon, \beta \ll 1, \tau \ll rc$, the current is

$$j(\tau)=(1-e^{-\epsilon/\beta})j_{OBC}(\tau)+\left(\frac{\epsilon(1-\tau)}{rc\sqrt{4\pi\beta\tau}}\right)(1+e^{-\epsilon/\beta})\exp\left(-\frac{(1-\tau)^2}{\beta\tau}\right). \quad \text{(B5)}$$

APPENDIX C: IMAGE DIFFUSION ANALYSIS WITH ABSORBING CATHODE AND ANODE

Appropriate initial images are[5,10]

$$\eta(\xi,0)=\eta_{OBC}(\xi-\epsilon,0)-e^{-\epsilon/\beta}\eta_{OBC}(\epsilon-\xi,0)+e^{1/\beta}\eta_{OBC}(\xi-2-\epsilon,0)-e^{(1-\epsilon)/\beta}\eta_{OBC}(2-\epsilon-\xi,0), \quad \text{(C1)}$$

The first two terms cancel for all time on the cathode boundary; the fourth term cancels the first term for all time on the anode boundary; and the third term cancels the second term for all time on the anode boundary. What is neglected is that the third and fourth terms produce a noncancelled contribution which for $\beta \ll 1$ is of order $e^{-2/\beta}$. One could add more images to take care of this but in view of the limitations of diffusion theory itself there is no point in so doing. Thus, unlike the one absorbing boundary case, no exact stipulation of the boundary conditions can be obtained from a finite number of image terms.

There have been two other ways of considering two absorbing boundary conditions. One is an *ad hoc* method of adding images.[17] The other is a direct series solution.[6] There has been some criticism of the first method on the grounds that some images do not satisfy the diffusion equation and are therefore not valid. This argument is faulty as sketched out (in the $rc \to 0$ limit) in Appendix D.

In order to connect with previous work[6,7] we shall indicate the results of three cases. For very short rise times and small diffusion, i.e., $rc \ll \gamma, \epsilon, \beta \ll 1, \tau$, the current transient is

$$j(\tau)=(1-e^{-\epsilon/\beta})\left[\tfrac{1}{2}\operatorname{erfc}\left(\frac{\tau-1}{\sqrt{4\beta\tau}}\right)-\left(\frac{\beta\tau}{\pi}\right)^{1/2}\left(\frac{1}{1+\tau}\right)\exp\left(-\frac{(1-\tau)^2}{4\beta\tau}\right)\right]-(1-e^{-\epsilon/\beta})\left(\frac{\epsilon}{\sqrt{4\pi\beta\tau}}\right)\exp\left(-\frac{(1-\tau)^2}{4\beta\tau}\right), \tag{C2}$$

which can give transients resembling Fig. 9. For intermediate rise time, i.e., $\gamma,\epsilon,\beta \ll 1,\tau,rc$, the current is

$$j(\tau)=(1-e^{-\epsilon/\beta})\left\{1-e^{-\tau/rc}+\tfrac{1}{2}\left[\exp\left(\frac{1-\tau}{rc}\right)-1\right]\operatorname{erfc}\left(\frac{1-\tau}{\sqrt{4\beta\tau}}\right)\right\}$$
$$-\frac{1}{rc}\left(\frac{\beta\tau}{\pi}\right)^{1/2}\exp\left(\frac{1-\tau}{rc}-\frac{(1-\tau)^2}{4\beta\tau}\right)\left((1+e^{-2/rc})-(1+e^{-\epsilon/\beta})\frac{\epsilon rc}{2\beta\tau}(1-e^{-2/rc})\right), \tag{C3}$$

and for long rise times, i.e., $\gamma,\epsilon,\beta \ll 1,\tau \ll rc$ the current is

$$j(\tau)=(1-e^{-\epsilon/\beta})j_{OBC}(\tau)-\frac{1}{rc}\left(\frac{\beta\tau}{\pi}\right)^{1/2}\left(1-e^{-\epsilon/\beta}-\frac{\epsilon}{2\beta\tau}(1+e^{-\epsilon/\beta})\right)\exp\left(-\frac{(1-\tau)^2}{4\beta\tau}\right). \tag{C4}$$

APPENDIX D: EIGENVALUE DIFFUSION ANALYSIS WITH ABSORBING CATHODE AND ANODE

Bernstein[6] starts with the transformation

$$\eta(\xi,\tau)=\eta(\xi)e^{-\gamma\tau},$$

where $\eta(\xi)$ satisfies

$$\beta\frac{\partial^2\eta}{\partial\xi^2}-\frac{\partial\eta}{\partial\xi}+\gamma\eta=0, \tag{D1}$$

subject to

$$\eta(0)=\eta(1)=0.$$

Then $\eta(\xi,\tau)$ is expanded in the eigenfunctions of Eq. (D1)

$$\eta_\lambda(\xi)=\sin(\lambda\pi\xi)e^{\xi/2\beta},$$

whose eigenvalues are

$$\gamma_\lambda=1/4\beta+\beta(\lambda\pi)^2.$$

The general solution to Eq. (2.6) is

$$\eta(\xi,\tau)=\sum_{\lambda=1}^{\infty}C_\lambda\eta_\lambda(\xi)e^{-\gamma\lambda\tau}.$$

Solving for the coefficient C_λ from the initial conditions,

$$\eta(\xi,\tau)=\exp\left(\frac{2\xi-2\epsilon-\tau}{4\beta}\right)\sum_{\lambda=1}^{\infty}\{\cos[\lambda\pi(\xi-\epsilon)]-\cos[\lambda\pi(\xi+\epsilon)]\}\exp(-\lambda^2\pi^2\beta\tau).$$

This can be converted into a much more rapidly converging series by use of a theta-function transformation.[6,19] The result is

$$n(\xi,\tau)=\frac{1}{4(\pi\beta)^{1/2}\tau}\exp\left(\frac{2\xi-2\epsilon-\tau}{4\beta}\right)\sum_{\sigma=-\infty}^{+\infty}\left[\exp\left(-\frac{(\xi-\epsilon+2\sigma)^2}{4\beta\tau}\right)+\exp\left(-\frac{(\xi-\epsilon-2\sigma)^2}{4\beta\tau}\right)\right.$$
$$\left.-\exp\left(-\frac{(\xi+\epsilon+2\sigma)^2}{4\beta\tau}\right)-\exp\left(-\frac{(\xi+\epsilon-2\sigma)^2}{4\beta\tau}\right)\right] \tag{D2}$$

or

$$\eta(\xi,\tau)=\eta_0(\xi-\epsilon,\tau)-\eta_0(\xi+\epsilon,\tau)e^{-\epsilon/\beta}$$
$$-\eta_0(\xi+\epsilon-2,\tau)e^{-\epsilon/\beta}+\eta_0(\xi-\epsilon-2,-\tau)+\cdots. \tag{D3}$$

Notice that the last two terms shown in Eq. (D3) travel in the direction opposite the drift and so do not satisfy Eq. (2.6) with $\gamma=0$. However, there is no reason why each term in a series solution to a linear differential equation need satisfy the equation. Only the sum need satisfy the equation. The theorem, that if every term of a series solution to a linear differential equation satisfies the equation, then the sum of the series also satisfies the equation, does not have a valid converse, as the counter example, Eq. (D3), shows.

Thus, the fact that Lucas[17] has images going in the $-v_d$ direction is not in itself incorrect, however the magnitudes of the images appear not correct when compared with the correct theory by Bernstein, i.e., Eq. (D2).

*Present address: Thermonuclear Division, Y-12, Oak Ridge National Laboratory, Oak Ridge, Tenn. 37830.
†Staff Member, Laboratory Astrophysics Division, National Bureau of Standards.
‡JILA Visiting Fellow, 1973–74. On leave from Dept. of Physics, Oregon State University, Corvallis, Ore. 97331.

[1]J. A. Hornbeck, Phys. Rev. 83, 374 (1951); 84, 615 (1951).
[2]M. A. Biondi and L. M. Chanin, Phys. Rev. 94, 910 (1954).
[3]Extension of the analysis of this paper to also include ionic motion, where the ions are generated by ionization, will be considered in a sequel paper, R. M. Stehman, R. J. Satterthwaitte, S.-P. Hong, S.-B. Woo, and J. H. Whealton (to be published).
[4]H. Raether, *Electron Avalanches and Breakdown in Gases* (Butterworths, London, 1964).
[5]J. J. Lowke, Aust. J. Phys. 15, 39 (1962).
[6]I. B. Bernstein, Westinghouse report No. 60-94439-I-A (1954) (unpublished); D. S. Burch (unpublished).
[7]L. G. H. Huxley and R. W. Crompton, *The Diffusion and Drift of Electrons in Gases* (Wiley, New York, 1974), Sec. 10.2.
[8]J. H. Whealton, E. F. Jaeger, and D. S. Burch, Phys. Rev. A 15, 773 (1977).
[9]E. W. McDaniel and E. A. Mason, *The Mobility and Diffusion of Ions in Gases* (Wiley, New York, 1973), Chap. 5.
[10]S. Chandraselshar, Rev. Mod. Phys. 15, 1 (1943).
[11]R. N. Varney, Phys. Rev. 98, 558 (1955); and private communication.
[12]D. S. Burch and J. H. Whealton (unpublished).
[13]D. Edelson, J. A. Morrison and K. B. McAfee, Jr., J. Appl. Phys. 36, 1682 (1964).
[14]J. Brambring, Z. Phys. 179, 532 (1964); H. Schlumbohm, Z. Phys. 182, 306 (1965) [English transl. available].
[15]A. Gilardini, *Low Energy Electron Collisions in Gases* (Wiley, New York, 1972), Chap. 3.
[16]R. N. Varney, Phys. Rev. 93, 1156 (1954); S. B. Woo, J. Chem. Phys. 42, 1251 (1965).
[17]J. Lucas, J. Electron. Control 17, 43 (1964).
[18]J. J. Thomson, *Conduction of Electricity Through Gases* (Cambridge U.P., Cambridge, 1928), p. 446 ff; L. B. Leob, *Basic Processes of Gaseous Electronics* (Berkeley U.P., Berkeley, Calif., 1955), p. 604 ff.
[19]R. Courant and D. Hilbert, *Methods of Mathematical Physics* (Wiley, New York, 1953), Vol. 1, p. 76; I. S. Gradshteyn and I. M. Ryzlirk, *Tables of Integrals, Series and Products* (Academic, New York, 1965).